

Advanced pneumonia classification using transfer learning on chest X-ray data with EfficientNet and ResNet

Green Arther Sandag, Timothy J. Mulalinda, Gloria A. M. Susanto, Stenly R. Pungus

Department of Informatics, Faculty of Computer Science, Klabat University, North Sulawesi, Indonesia

Article Info

Article history:

Received Jun 9, 2024

Revised Jun 26, 2025

Accepted Aug 1, 2025

Keywords:

Deep learning

EfficientNet

ResNet

Transfer learning

X-ray

ABSTRACT

Pneumonia is a serious lung infection that demands accurate and timely diagnosis to reduce mortality. This study explores the use of deep learning and transfer learning for classifying chest X-ray images into two categories: normal and pneumonia. A total of 5,632 labeled images were used to train and evaluate six pre-trained convolutional neural network (CNN) architectures: EfficientNetB1, B3, B5, B7, ResNet50, and ResNet101. The models were tested across three training scenarios by varying learning rates (LR), batch sizes, and epochs. Among all models, EfficientNetB3 achieved the highest performance, with accuracy of 99.04%, precision of 99.76%, recall of 99.23%, and F1-score of 99.34%. These results indicate that EfficientNetB3 offers a robust and efficient solution for pneumonia detection. This research contributes to the development of intelligent diagnostic tools in the medical field and provides practical guidance for selecting effective deep learning models in clinical imaging applications.

This is an open access article under the [CC BY-SA](#) license.



Corresponding Author:

Green Arther Sandag

Department of Informatics, Faculty of Computer Science, Klabat University

Arnold Mononutu, North Sulawesi 95371, Indonesia

Email: greensandag@unklab.ac.id

1. INTRODUCTION

An illness that affects one or both lungs is known as pneumonia, or inflammation of the lungs [1]. This leads to the alveoli, or air sacs, where pus or fluid is released from the lungs. Pneumonia can be brought on by fungus, viruses, or bacteria. The illness can cause mild to severe symptoms, such as fever, chills, coughing up blood or mucus, and trouble breathing [2]. Pneumonia, one of the most prevalent acute lower respiratory tract infections, continues to pose a major global health challenge, with an estimated 489 million new cases reported worldwide in 2019 [3]. Every hour, two to three children in Bangladesh die from pneumonia, which also stands as the primary cause of hospitalization in those under five [4]. However, it is also important to note that technology in diagnosing and monitoring lung diseases, especially in dealing with conditions like pneumonia, plays a significant role. Lung X-rays are a method used for the initial classification and evaluation of pneumonia. The process of diagnosing pneumonia involves using electromagnetic wave radiation to obtain image results of the lungs [5].

The advancement of artificial intelligence (AI), particularly in machine learning and deep learning, has greatly improved the classification of pneumonia in X-ray images through the use of convolutional neural networks (CNNs) [6]. Deep learning enables computers to understand complex patterns in data by utilizing layered neural networks (multi layer neural network) [7]. By employing deep learning methods such as CNNs, effectiveness in image classification tasks is achieved because the number of parameters and connections required in these networks is much lower compared to other types of neural networks. This advantage simplifies the neural network CNN training process compared to the use of other neural networks [8].

However, producing accurate CNN models often requires large datasets and significant computational time to train them. Therefore, transfer learning techniques become relevant in the development of CNN models for pneumonia classification. By utilizing transfer learning, existing CNN models can be leveraged to learn features from large datasets, such as shapes or textures, to aid in the process of pneumonia classification and diagnosis [9]. Transfer learning is a technique in machine learning where a pre-trained model can be used to solve different problems without retraining from scratch [10]. This model leverages prior knowledge from a large dataset but can also be applied to smaller datasets. Transfer learning involves extracting knowledge from multiple source tasks and applying it to a different target task. Unlike multitasking learning, which considers both the source and target tasks simultaneously, transfer learning focuses solely on the target task. The symmetry between the source and target tasks is not mandatory in transfer learning [11].

In our study, we utilized gradient-weighted class activation mapping (Grad-CAM), a technique within CNNs, to generate class-specific heatmaps. These heatmaps are tailored to a specific input image, leveraging a trained CNN model [12], [13]. The Grad-CAM technique is employed to enhance pneumonia detection transparency [14]. It highlights regions in the input image where the model focuses during classification, indicating that feature maps in the final convolution layer retain spatial information crucial for capturing visual patterns. These patterns aid in distinguishing assigned classes. Grad-CAM utilizes layers and extracted features from the trained model to achieve this [12]. In a study conducted by Cha *et al.* [15], they aimed to classify pneumonia in chest X-ray images using attention-based transfer learning. Researchers combined feature vectors from three pre-trained models: ResNet152, DenseNet121, and ResNet18. The best result was achieved with squeeze-and-excitation (SE), with an accuracy of 96.63%, F1-score of 0.973, area under the curve (AUC) of 96.03%, precision of 96.24%, and recall of 98.46%. Mahin *et al.* [16] conducted research on the use of transfer learning for the classification of COVID-19 and pneumonia in chest X-ray images. Researchers used four different transfer learning algorithms, including MobileNetV2, VGG19, Inceptionv3, and EffNet threshold, to train pre-trained models in transfer learning. In this study, the highest accuracy achieved was 98% using the MobileNetV2 algorithm, followed by Inceptionv3 with 96.92%, EffNet threshold with 94.95%, and VGG19 with 92.82%.

The study aims to develop and evaluate a pneumonia classification model using lung X-ray images by integrating transfer learning techniques and implementing the model into a web application capable of classifying into two classes: pneumonia and normal. The tested models include EfficientNet B1, EfficientNet B3, EfficientNet B5, EfficientNet B7 [17], ResNet50, and ResNet101 [18], using a dataset from the Guangzhou Women and Children's Medical Center obtained from Kaggle [19].

2. METHOD

In this research design, the data used consists of the chest X-ray images (pneumonia) dataset obtained from Kaggle [19]. The data will be processed using various feature extraction techniques to convert features into a format suitable for further analysis. By integrating transfer learning architectures such as EfficientNetB1, B3, B5, B7, ResNet50, and ResNet101, the model learning process will be faster and more efficient in classifying lung X-ray images into two classes: pneumonia and normal. The models will be evaluated using a confusion matrix to determine performance metrics, including accuracy, recall, precision, and F1-score. A comparative analysis will be conducted among the six models to identify the most optimal one based on performance. The selected model will then be implemented into a web application. After deployment, all feature functions will be tested to address potential errors. The web application will allow users to upload X-ray images, and the integrated model will classify the images into the two classes, displaying the output image along with probability percentage values. The entire process flow is illustrated in Figure 1.

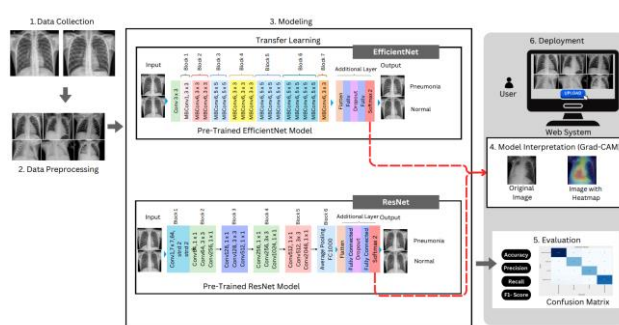


Figure 1. Proposed methodology for detecting pneumonia

2.1. Data collection

We utilized the chest X-ray images (pneumonia) dataset, comprising a total of 5,856 image samples. This dataset was then divided into 1,583 images of normal lungs and 4,273 images of lungs affected by pneumonia. The division was distributed into three folders: data test, data train, and data valid. Data test contained 234 normal lung images and 390 pneumonia lung images, data train consisted of 1,341 normal lung images and 3,875 pneumonia lung images, while data valid comprised 8 normal lung images and 8 pneumonia lung images. To address this issue, we adjusted the data test by equalizing the number of normal and pneumonia images to 200 for each class. Details of the dataset are in Figure 2.

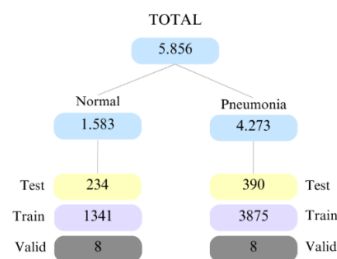


Figure 2. Details of the total image

2.2. Data preprocessing

In this stage, we will prepare the adjusted image data before using it for model training. The initial step involves reading the folder structure of the data containing chest X-ray lung images, which have been divided into two classes: normal and pneumonia. The image data will be organized into a dataframe, indicating their respective classes. Next, the dataframe will be divided into three parts: training data, testing data, and validation data, with appropriate proportions for each part. The image sizes will be adjusted to 224×224 pixels and will be processed in red, green, and blue (RGB) mode. Subsequently, a data generator will be created using the ImageDataGenerator library from Keras to load the data gradually during the model training process [20]. Additionally, the batch size for the testing data will be dynamically adjusted to match the available data, maximizing memory usage and processing efficiency. Furthermore, there will be some samples from the training data along with their classes which are plotted as in Figure 3.

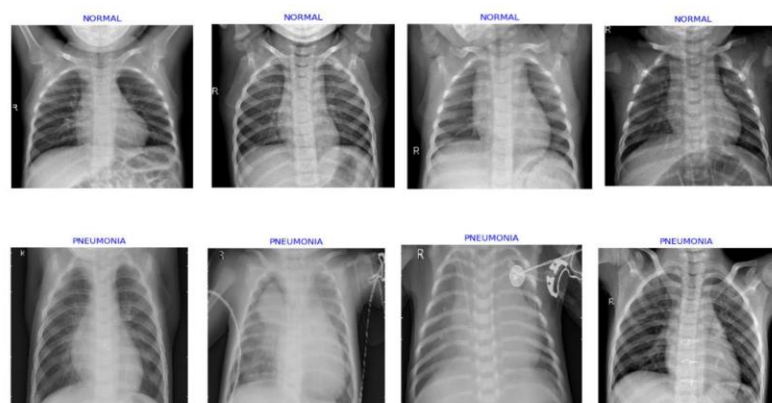


Figure 3. Sample of training data

2.3. Modeling

The upcoming stage of the deep learning process will utilize CNN techniques, leveraging transfer learning from the EfficientNet and ResNet architectures. EfficientNet is designed for image recognition and classification, emphasizing resource efficiency by optimizing the number of parameters and computations. It uses scaling methods to adjust the CNN dimensions of depth, width, and resolution with a compound

coefficient [21]. ResNet, or residual neural network (RNN), addresses the vanishing gradient problem in deep networks by incorporating skip connections, enabling more effective feature learning and preventing performance degradation in very deep networks [22]. Both architectures will be adjusted: the convolution layer and max pooling will be retained, while the flatten, fully connected, and dropout layers will be modified to produce a softmax output with 2 classes: pneumonia and normal.

Table 1 presents the parameter settings used in each of the three experimental scenarios. Each scenario involved training models with different configurations of epoch count, learning rate (LR), and batch size while keeping the loss function (categorical) and optimizer types (AdaMax, stochastic gradient descent (SGD), and RMSprop) consistent across the scenarios. These variations were designed to evaluate the performance impact of training duration and hyperparameter adjustments across multiple deep learning architectures including EfficientNetB1, EfficientNetB3, EfficientNetB5, EfficientNetB7, ResNet50, and ResNet101.

Table 1. Parameters of each scenario

Scenario	Optimizer	Epoch	LR	Loss function	Batch size
1	AdaMax, SGD, and RMSprop	20	0.001	Categorical	16
2	AdaMax, SGD, and RMSprop	30	0.001	Categorical	20
3	AdaMax, SGD, and RMSprop	30	0.01	Categorical	45

In the next step, we conducted modeling experiments using EfficientNetB1, EfficientNetB3, EfficientNetB5, EfficientNetB7, ResNet50, and ResNet101. The model creation process was divided into three scenarios, each with variations in optimizer, epochs, LR, loss function, and batch size. In the first scenario, we used AdaMax, SGD, and RMSProp as optimizers, with 20 epochs, LR 0.001, categorical loss function, and a batch size of 16. The second scenario also employed AdaMax, SGD, and RMSProp as optimizers, with 30 epochs, LR 0.001, categorical loss function, and a batch size of 20. The third scenario utilized AdaMax, SGD, and RMSProp as optimizers, with 30 epochs, LR 0.01, categorical loss function, and a batch size of 45.

2.3.1. EfficientNet

The EfficientNet algorithm was initially presented by Tan and Le [22], which provides a novel approach to scaling neural network models by improving depth, width, and precision. It is a CNN design and scaling method that uniformly increases the depth, breadth, and resolution dimensions by using a compounded coefficient. EfficientNet introduces a novel approach to scaling models by using a coefficient that simultaneously increases the network's depth, width, and resolution. Unlike conventional scaling methods, which often modify only one or two dimensions, EfficientNet ensures that all dimensions are proportionally enhanced. This approach allows the model to achieve higher performance with better computational efficiency [21].

2.3.2. ResNet

The ResNet architecture introduces skip (residual) connections which facilitate the flow of gradients through alternative paths, solving the problem of vanishing gradients in deep neural networks. With residual blocks, training deep networks becomes more efficient. ResNet also offers flexibility in the number of layers, like ResNet-18 consisting of 18 layers, ResNet-34 with 34 layers, and ResNet-50 with 50 layers. Nevertheless, as the number of layers increases, it leads to a higher usage of parameters [23].

2.4. Model interpretation

Next, model interpretation will be applied to the normal and pneumonia image data to highlight the pneumonia area in the lung X-ray images [24]. This will be done using the Grad-CAM technique, which leverages gradients from the last CNN layer to identify important areas in making predictions [25]. The result, called the HeatMap, is a visual representation of the activation intensity in the convolutional layers of the neural network while processing the images [26].

2.5. Evaluation

In the evaluation stage, we will use a confusion matrix to assess the classification of image [27], aiming to compute performance metrics such as accuracy, precision, recall, and F1-score from the utilized dataset. Accuracy indicates the model's ability to classify data correctly. Precision characterizes the agreement between requested data and the model's predicted outcomes. Recall illustrates the model's capability to retrieve specific information. On the other hand, the F1-score represents the balanced average of precision and recall. The formulas utilized to compute performance metrics is:

$$\text{Accuracy} = \frac{(TP+TN)}{(TP+FP+FN+TN)} \quad (1)$$

$$\text{Precision} = \frac{TP}{(FP+TP)} \quad (2)$$

$$\text{Recall} = \frac{TP}{(TP+FN)} \quad (3)$$

$$\text{F1 score} = \frac{(2 \times \text{Recall} \times \text{Precision})}{(\text{Recall} + \text{Precision})} \quad (4)$$

The purpose of evaluation is to measure which model exhibits the best performance. This provides a comprehensive overview of how well the models classify data and is highly useful in assessing binary classification models.

2.6. Deployment

The final stage, we will create a straightforward web system application to perform pneumonia classification on lung X-ray image data. This web application is designed to predict or classify lung X-ray images uploaded by users. The output will display the probability and classification of whether the image belongs to the “pneumonia” or “normal” class.

3. RESULTS AND DISCUSSION

We conducted our experiments using two architectural models, EfficientNet and ResNet. In the following subsections, we report the results.

3.1. Analysis of optimal model performance across different scenarios

Table 2 presents the best-performing models across three training scenarios using AdaMax, SGD, and RMSprop optimizers. In scenario 1, the combination of AdaMax and EfficientNetB3 achieved the most outstanding performance, with an accuracy of 99.04%, precision of 99.76%, recall of 99.23%, and F1-score of 99.34%. This indicates a highly balanced model with minimal false positives and false negatives. While SGD and RMSprop also performed well with EfficientNetB7, their performance was slightly lower, especially in terms of Precision for RMSprop. In scenario 2, EfficientNetB3 again demonstrated superior consistency, particularly when trained using AdaMax and RMSprop, both yielding an accuracy of 99.04% and high F1-scores (99.14% and 99.55%, respectively).

Table 2. Best models from each scenario

Scenario	Optimizer	Model	Accuracy	Precision	Recall	F1-score
1	AdaMax	EfficientNetB3	99.04%	99.76%	99.23%	99.34%
	SGD	EfficientNetB7	98.32%	98.84%	98.12%	98.55%
	RMSprop	EfficientNetB7	98.56%	97.45%	99.11%	98.11%
2	AdaMax	EfficientNetB3	99.04%	98.34%	99.02%	99.14%
	SGD	ResNet50	98.32%	97.22%	98.84%	98.43%
	RMSprop	EfficientNetB3	99.04%	98.53%	99.02%	99.55%
3	Adamax	EfficientNetB1	96.88%	94.87%	98.11%	96.22%
	SGD	EfficientNetB3	99.04%	98.46%	99.23%	99.11%
	RMSprop	EfficientNetB1	97.84%	98.88%	96.44%	97.18%

The graphs in Figure 4 show the training and validation loss and accuracy for three scenarios: Figures 4(a)-(c). In scenario 1, both training and validation losses decrease steadily and converge, indicating effective learning with minimal overfitting. The best epoch is marked at 20 for loss and 17 for accuracy, showing optimal performance. Scenario 2 follows a similar trend, with losses converging and the best epoch at 23, reflecting stable learning and robust performance. Both scenarios show consistent improvements in training and validation accuracy, with near-perfect training accuracy and slightly fluctuating but high validation accuracy. In contrast, scenario 3 exhibits significant fluctuations in training loss and an increasing validation loss after the best epoch at 3, indicating overfitting. Its accuracy trends are unstable, with rapid training accuracy improvements but fluctuating validation accuracy. This suggests scenario 3 could benefit from additional regularization to improve generalization. Overall, scenarios 1 and 2 perform better with minimal overfitting, while scenario 3 highlights challenges in maintaining stability and preventing overfitting. These findings underscore the importance of selecting the right epoch to balance accuracy and generalization for robust model performance.

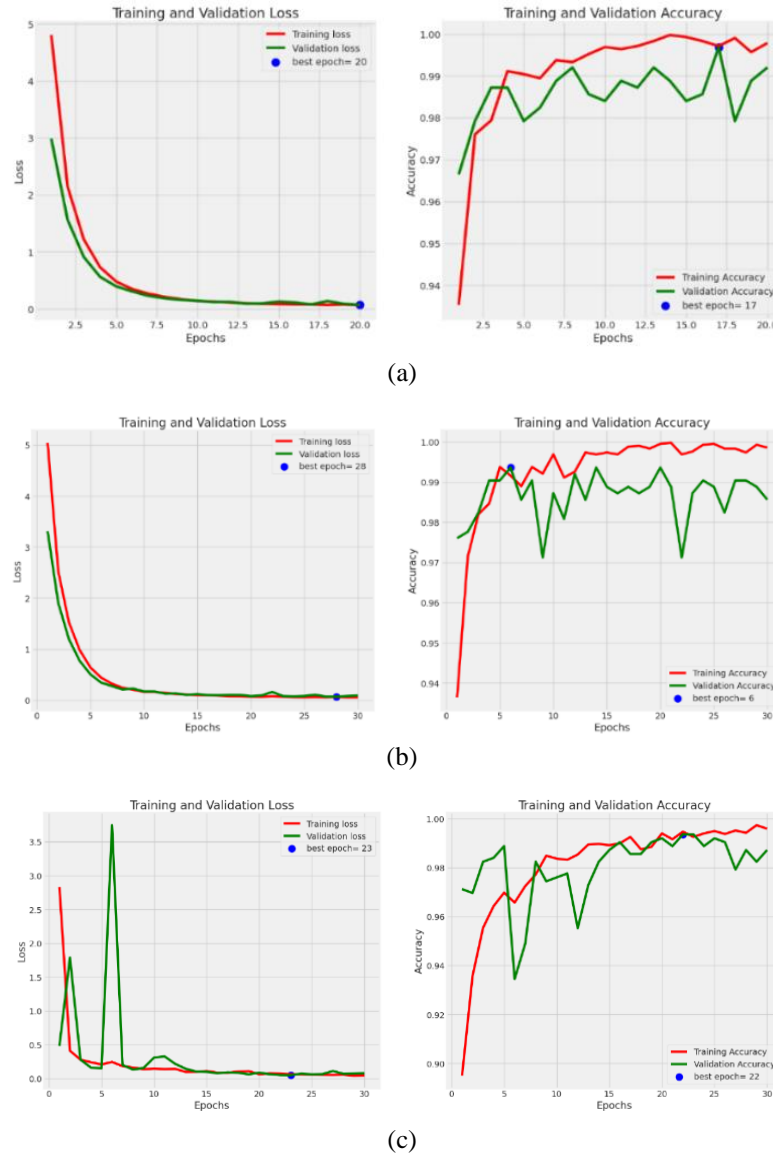


Figure 4. Training and validation loss and accuracy graphs for three different scenarios labeled; (a) scenario 1, (b) scenario 2, and (c) scenario 3

3.2. Comparison with related research

In order to establish the comparative effectiveness of our proposed approach, we benchmarked its performance against previously reported transfer learning models on chest X-ray image classification for pneumonia detection. Table 3 shows that our model outperforms four other models in terms of accuracy. Jain *et al.* [8] used models like 2 convolutional layer, 3 convolutional layer, VGG16, VGG19, ResNet50, and Inception-v3 on the chest X-ray images (pneumonia) dataset, achieving the best accuracy of 92.31% with 3 convolutional layer using categorical classification. Kalgutkar *et al.* [28] employed VGG16, ResNet50, and InceptionV3 on the labeled optical coherence tomography and chest X-ray images classification dataset, with VGG16 reaching the highest accuracy of 94% using binary classification. Chatterjee *et al.* [29] used VGG16, VGG19, ResNet50, MobileNetV1, and EfficientNetB3 on the chest X-ray images (pneumonia) dataset, where EfficientNetB3 achieved the best accuracy of 93% with binary classification. Similarly, Niño *et al.* [30] utilized DenseNet, VGG19, and ResNet50 on the same dataset, with ResNet50 achieving the highest accuracy of 91% using binary classification. In contrast, our model, EfficientNetB3, achieved an accuracy rate of 99.04% in categorical classification on the chest X-ray images (pneumonia) dataset. This indicates that our model is more accurate than the others, highlighting its effectiveness for precise pneumonia detection.

Table 3. Model comparison with related research

Reference	Model	Dataset	Best model accuracy result	Classification method
Jain <i>et al.</i> [8]	2 convolutional layer, 3 convolutional layer, VGG16, VGG19, ResNet50, and Inception-v3	Chest X-ray images (pneumonia)	3 convolutional layer (92.31%)	Categorical
Kalgutkar <i>et al.</i> [28]	VGG16, ResNet50, and InceptionV3	Labeled optical coherence tomography and chest X-ray images classification	VGG16 (94%)	Binary
Chatterjee <i>et al.</i> [29]	VGG16, VGG19, ResNet50, MobileNetV1, and EfficientNetB3	Chest X-ray images (pneumonia)	EfficientNetB3 (93%)	Binary
Niño <i>et al.</i> [30]	DenseNet, VGG19, and ResNet50	Chest X-ray images (pneumonia)	ResNet50 (91%)	Binary
Our research	EfficientNet (B1, B3, B5, and B7), and ResNet (50 and 101)	Chest X-ray images (pneumonia)	EfficientNetB3 (99.04%)	Categorical

3.3. Grad-CAM visualization

This section explains the results of applying the Grad-CAM algorithm to the previously tested top-performing model, EfficientNetB3. This model highlights specific areas in images, such as regions affected by pneumonia in lung X-rays, allowing for more accurate diagnostic information. The explainable deep learning algorithm, custom Grad-CAM, retrieves information from the final convolutional layer and transforms it into a heatmap. The heatmap displays regions that the classifier focused on to reach its conclusion. Red and yellow areas on the heatmap indicate the lung regions most relevant to the model's pneumonia prediction, with color intensity reflecting the level of importance. The image in Figure 5 shows a standard chest X-ray, while the image below it overlays the Grad-CAM heatmap. This heatmap assists radiologists and medical professionals in concentrating on areas likely affected by pneumonia, facilitating quicker and more accurate diagnoses. By overlaying the heatmap on the original image, healthcare professionals can assess the factors influencing the decision, ensuring a more informed and reliable diagnostic process. The effectiveness of the Grad-CAM heatmap in identifying pneumonia-affected regions can be validated against clinical findings, ensuring the model's reliability in a clinical setting.

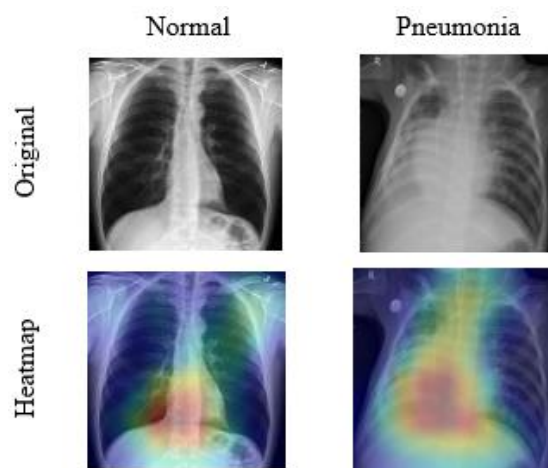


Figure 5. Grad-CAM of pneumonia lung images

3.4. Pneumonia classification web system

To translate the research findings into a practical tool, the developed model was integrated into a simple web-based system. In Figure 6, the final stage after completing model development and evaluation is the design of this web application to test the trained model. This web system enables users to upload chest X-ray images directly through the interface, providing an accessible way to interact with the classifier. Once the image is uploaded, the model automatically processes it and classifies the result into one of two categories: normal or pneumonia, thereby demonstrating the practical deployment of the system.

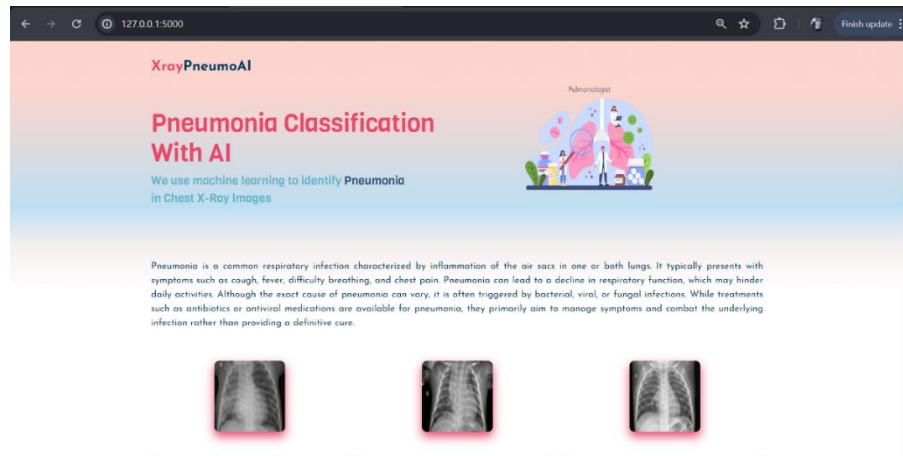


Figure 6. Pneumonia classification web system

4. CONCLUSION

The utilization of CNN for classifying lung X-ray images into normal and pneumonia categories can be integrated by leveraging transfer learning techniques such as EfficientNet and ResNet, and then implemented into a Web App. EfficientNetB3 demonstrated the most optimal and best performance with an accuracy of 99.04%, using a LR of 0.001, batch size of 20, and 30 epochs, along with categorical loss function and AdaMax optimizer. This model outperformed EfficientNetB1, B5, B7, ResNet50, and ResNet101 models. Overall, this research found that the application of CNN with transfer learning model EfficientNetB3 is a highly promising choice, offering strong potential as a solution for classifying pneumonia lung X-ray images.

ACKNOWLEDGMENTS

The author gratefully acknowledges the Faculty of Computer Science, Klabat University, for its continuous support and encouragement throughout the completion of this research. The academic environment and research facilities provided by the faculty have been essential in facilitating this study.

FUNDING INFORMATION

This research was supported by Klabat University.

AUTHOR CONTRIBUTIONS STATEMENT

This journal uses the Contributor Roles Taxonomy (CRediT) to recognize individual author contributions, reduce authorship disputes, and facilitate collaboration.

Name of Author	C	M	So	Va	Fo	I	R	D	O	E	Vi	Su	P	Fu
Green Arther Sandag	✓	✓	✓	✓		✓		✓	✓	✓	✓		✓	✓
Timothy J. Mulalinda		✓		✓	✓	✓		✓		✓	✓	✓		
Gloria A. M. Susanto	✓		✓	✓			✓			✓	✓	✓	✓	
Stenly R. Pungus	✓	✓		✓	✓	✓	✓	✓	✓		✓			✓

C : **C**onceptualization

M : **M**ethodology

So : **S**oftware

Va : **V**alidation

Fo : **F**ormal analysis

I : **I**nterpretation

R : **R**esources

D : **D**ata Curation

O : **O**riginal Draft

E : **E**diting

Vi : **V**isualization

Su : **S**upervision

P : **P**roject administration

Fu : **F**unding acquisition

CONFLICT OF INTEREST STATEMENT

The author declares that there is no conflict of interest regarding the publication of this paper.

INFORMED CONSENT

We used the dataset available on the Kaggle website, so we have obtained informed consent from all individuals included in this study.

ETHICAL APPROVAL

This study did not involve any human participants or animals. Therefore, ethical approval was not required.

DATA AVAILABILITY

The data that support the findings of this study are openly available in Kaggle at <https://www.kaggle.com/datasets/paultimothymooney/chest-xray-pneumonia> [19].




REFERENCES

- [1] V. Kumar, "Pulmonary innate immune response determines the outcome of inflammation during pneumonia and sepsis-associated acute lung injury," *Frontiers in Immunology*, vol. 11, p. 1722, 2020, doi: 10.3389/fimmu.2020.01722.
- [2] National Heart, Lung, and Blood Institute, "What is pneumonia?," NIH. Accessed: Sep. 14, 2023. [Online]. Available: <https://www.nhlbi.nih.gov/health/pneumonia>
- [3] D. Feng *et al.*, "Clinical trial landscape for pneumonia: Evolving agents against bacterial pathogens," *International Journal of Infectious Diseases*, vol. 158, 2025, doi: 10.1016/j.ijid.2025.107965.
- [4] S. B. Zaman, N. Hossain, Md. T. U. S. Talha, K. Hasan, R. B. Zaman, and R. Khan, "Assessing the risk of antibiotic resistance in childhood pneumonia: A hospital-based study in Bangladesh," *Healthcare*, vol. 13, no. 3, p. 207, Jan. 2025, doi: 10.3390/healthcare13030207.
- [5] A. Nathani and H. E. Dincer, "Advancements in imaging technologies for the diagnosis of lung cancer and other pulmonary diseases," *Diagnostics*, vol. 15, no. 7, p. 826, Mar. 2025, doi: 10.3390/diagnostics15070826.
- [6] K. M. Abubeker and S. Baskar, "B2-Net: An artificial intelligence powered machine learning framework for the classification of pneumonia in chest X-ray images," *Machine Learning: Science and Technology*, vol. 4, no. 1, Apr. 2023, doi: 10.1088/2632-2153/acc30f.
- [7] I. H. Sarker, "Deep learning: A comprehensive overview on techniques, taxonomy, applications and research directions," *SN Computer Science*, vol. 2, no. 6, Aug. 2021, doi: 10.1007/s42979-021-00815-1.
- [8] R. Jain, P. Nagrath, G. Kataria, V. S. Kaushik, and D. J. Hemanth, "Pneumonia detection in chest X-ray images using convolutional neural networks and transfer learning," *Measurement*, vol. 165, p. 108046, 2020, doi: 10.1016/j.measurement.2020.108046.
- [9] M. Patel, A. Sojitra, Z. Patel, and M. H. Bohara, "Pneumonia detection using transfer learning," *International Journal of Engineering Research & Technology (IJERT)*, vol. 10, no. 10, pp. 252–261, 2021.
- [10] E. Baykal, H. Dogan, M. E. Ercin, S. Ersoz, and M. Ekinici, "Transfer learning with pre-trained deep convolutional neural networks for serous cell classification," *Multimedia Tools and Applications*, vol. 79, pp. 15593–15611, Jun. 2020, doi: 10.1007/s11042-019-07821-9.
- [11] P. Chhikara, P. Singh, P. Gupta, and T. Bhatia, "Deep convolutional neural network with transfer learning for detecting pneumonia on chest X-rays," *Advances in Intelligent Systems and Computing*, vol. 1064, pp. 155–168, 2020, doi: 10.1007/978-981-15-0339-9_13.
- [12] G. A. Sandag and R. Maringka, "Utilizing transfer learning for brain tumor detection and grad-CAM visual explanation," *2024 6th International Conference on Cybernetics and Intelligent System (ICORIS). IEEE*, 2024, pp. 1–6, doi: 10.1109/icoris63540.2024.10903960.
- [13] R. R. Selvaraju, M. Cogswell, A. Das, R. Vedantam, D. Parikh, and D. Batra, "Grad-CAM: Visual explanations from deep networks via gradient-based localization," *International Journal of Computer Vision*, vol. 128, no. 2, pp. 336–359, 2020, doi: 10.1007/s11263-019-01228-7.
- [14] M. K. U. Ahamed *et al.*, "DTLCx: An improved resnet architecture to classify normal and conventional pneumonia cases from COVID-19 instances with Grad-CAM-based superimposed visualization utilizing chest X-ray images," *Diagnostics*, vol. 13, no. 3, p. 551, 2023, doi: 10.3390/diagnostics13030551.
- [15] S. -M. Cha, S. -S. Lee, and B. Ko, "Attention-based transfer learning for efficient pneumonia detection in chest X-ray images," *Applied Sciences*, vol. 11, no. 3, p. 1242, 2021, doi: 10.3390/app11031242.
- [16] M. Mahin, S. Tonmoy, R. Islam, T. Tazin, M. M. Khan, and S. Bourouis, "Classification of COVID-19 and pneumonia using deep transfer learning," *Journal of Healthcare Engineering*, vol. 2021, no. 1, pp. 1–11, 2021, doi: 10.1155/2021/3514821.
- [17] Y. Y. Arun and G. S. Viknesh, "Leaf classification for plant recognition using EfficientNet architecture," *2022 IEEE Fourth International Conference on Advances in Electronics, Computers and Communications (ICAEECC)*, Bengaluru, India, 2022, pp. 1–5, doi: 10.1109/ICAEECC54045.2022.9716637.
- [18] T. Tuncer, F. Ertam, S. Dogan, E. Aydemir, and P. Plawiak, "Ensemble residual network-based gender and activity recognition method with signals," *The Journal of Supercomputing*, vol. 76, pp. 2119–2138, 2020, doi: 10.1007/s11227-020-03205-1.
- [19] P. Mooney, "Chest X-ray images (Pneumonia)," *Kaggle*, 2018. [Online]. Available: <https://www.kaggle.com/datasets/paultimothymooney/chest-xray-pneumonia>
- [20] N. Arora and M. M. Abraham, "Leveraging convolutional neural networks for face mask detection," *2022 Fifth International Conference on Computational Intelligence and Communication Technologies (CCICT)*, Sonapat, India, 2022, pp. 418–421, doi: 10.1109/CCICT56684.2022.00080.
- [21] A. S. Ebenezer, S. D. Kanmani, M. Sivakumar, and S. J. Priya, "Effect of image transformation on EfficientNet model for COVID-19 CT image classification," *Materialstoday: Proceedings*, vol. 51, pp. 2512–2519, 2022, doi: 10.1016/j.matpr.2021.12.121.
- [22] M. Tan and Q. V. Le, "EfficientNet: Rethinking model scaling for convolutional neural networks," *arXiv:1905.11946*, 2019, doi:




- 10.48550/arXiv.1905.11946.
- [23] S. A. Hasanah, A. A. Pravitasari, A. S. Abdullah, I. N. Yulita, and M. H. Asnawi, "A deep learning review of ResNet architecture for lung disease identification in CXR image," *Applied Sciences*, vol. 13, no. 24, p. 13111, 2023, doi: 10.3390/app132413111.
 - [24] C. O. Toro, A. G. Pedrero, M. L. Saavedra, and C. G. Martín, "Automatic detection of pneumonia in chest X-ray images using textural features," *Computers in Biology and Medicine*, Elsevier, vol. 145, p. 105466, 2022, doi: 10.1016/j.compbiomed.2022.105466.
 - [25] S. Soomro, A. Niaz and K. Nam Choi, "Grad++ScoreCAM: Enhancing visual explanations of deep convolutional networks using incremented gradient and score-weighted methods," in *IEEE Access*, vol. 12, pp. 61104-61112, 2024, doi: 10.1109/ACCESS.2024.3392853.
 - [26] L. Visuña, D. Yang, J. G. Blas, and J. Carretero, "Computer-aided diagnostic for classifying chest X-ray images using deep ensemble learning," *BMC Med. Imaging*, vol. 22, no. 1, pp. 1-17, 2022, doi: 10.1186/s12880-022-00904-4.
 - [27] N. E. Ramli, Z. R. Yahya, and N. A. Said, "Confusion matrix as performance measure for corner detectors," *Journal of Advanced Research in Applied Sciences and Engineering Technology*, vol. 29, no. 1, 2022, doi: 10.37934/araset.29.1.256265.
 - [28] S. Kalgutkar *et al.*, "Pneumonia detection from chest X-ray using transfer learning," *2021 6th International Conference for Convergence in Technology (I2CT)*, Maharashtra, India, 2021, pp. 1-6, doi: 10.1109/I2CT51068.2021.9417872.
 - [29] R. Chatterjee, A. Chatterjee, and R. Halder, "An efficient pneumonia detection from the Chest X-Ray images," *Proceedings of International Conference on Machine Intelligence and Data Science Applications*, Springer, Singapore, pp. 779-789, 2021, doi: 10.1007/978-981-33-4087-9_63.
 - [30] G. L. E. M. Niño, J. G. N. Fernandez, F. Y. T. Calderon, I. A. Olano, P. D. L. Cruz, and G. C. Barco, "Classification model using transfer learning for the detection of pneumonia in chest X-Ray images," *International Journal of Online and Biomedical Engineering (iJOE)*, vol. 20, no. 5, pp. 150-161, Mar. 2024, doi: 10.3991/ijoe.v20i05.45277.

BIOGRAPHIES OF AUTHORS






Green Arther Sandag    received a Bachelor's degree in Computer Science from Universitas Klabat, Airmadidi, Indonesia, in 2012, and a Master's degree in Computer Science from Yuan Ze University, Taoyuan, Taiwan, in 2016. Since August 2016, he has been working as a lecturer at Universitas Klabat, Airmadidi, Indonesia. His research interests include computer vision and natural language processing, with a particular focus on topics such as sentiment analysis, emotion classification, and image classification. He can be contacted at email: greensandag@unklab.ac.id.






Timothy J. Mulalinda    was born in Bitung on November 30, 2003. After completing secondary education, continued undergraduate studies at Universitas Klabat, focusing on informatics. During their time as a student, they learned extensively and enhanced their skills in technology and software development. They participated in various projects and activities related to technology, further strengthening their abilities in the field. He can be contacted at email: s2200056@student.unklab.ac.id.



Gloria A. M. Susanto    was born in Manado on August 15, 2002. After completing secondary education, she pursued an undergraduate degree at Universitas Klabat, focusing on Informatics. During her college years, she dedicated significant time to studying and honing her skills in technology and software development. She believes that the education she has received will provide a strong foundation for her career in the tech industry. She can be contacted at email: s2200057@student.unklab.ac.id.



Stenly R. Pungus    Dean and Lecturer in the Computer Science Faculty at Klabat University, Airmadidi, Manado. He holds a Ph.D. in Data Modelling from the National University of Malaysia, where his research focused on advanced techniques for structuring and analyzing complex data systems. He is also an alumnus of the Master's program in Software Engineering from the Bandung Institute of Technology and hold a Master's degree in Management from Klabat University. He can be contacted at email: stenly.pungus@unklab.ac.id.